A class of exact two-dimensional kinetic current sheet equilibria

Peter H. Yoon
Institute for Physical Science and Technology, University of Maryland, College Park, Maryland, USA

Anthony T. Y. Lui
Johns Hopkins University Applied Physics Laboratory, Laurel, Maryland, USA

Received 27 October 2003; revised 2 July 2004; accepted 19 October 2004; published 7 January 2005.

[1] The present paper discusses a class of exact two-dimensional kinetic current sheet equilibria. The general solution to the two-dimensional Grad-Shafranov equation was first obtained by Walker in 1915 in terms of the generating function $g(\zeta)$ ($\zeta = X + iZ$), where X and Z are two dimensionless spatial coordinates. There are infinite choices of $g(\zeta)$, but not every solution yields physically meaningful or mathematically useful form. The known solutions to date with geophysical application include those by *Harris* [1962], *Fadeev et al.* [1965], *Kan* [1973], *Manankova et al.* [2000], and *Brittnacher and Whipple* [2002]. In this paper, these solutions are reviewed systematically, and several new solutions are proposed. These include a generalization of the Harris-Fadeev-Kan-Manankova line of model, a model for an isolated X-line alternative to that of Brittnacher-Whipple, and finally a model which represents an isolated magnetic island.

Citation: Yoon, P. H., and A. T. Y. Lui (2005), A class of exact two-dimensional kinetic current sheet equilibria, *J. Geophys. Res.*, *110*, A01202, doi:10.1029/2003JA010308.

1. Introduction

[2] The study of current sheet equilibria which separates two regions of oppositely directed magnetic fields has been an important research topic in space plasma physics research since *Ness* [1965] reported the discovery of current sheet in the magnetotail. It has applications in several frontier research areas. Thin current sheet structure has been inferred at the Sun [*Solanki et al.*, 2003]. It is also observed in the heliosphere [*Burton et al.*, 1994], in the Earth's and other planetary magnetospheres [*Ness*, 1965, 1987], as well as in comets [*Siscoe et al.*, 1986].

[3] One of the most widely used current sheet models is the Harris equilibrium [*Harris*, 1962], which is an exact one-dimensional solution to kinetic Vlasov-Maxwell equilibrium equation. Over the years, there have been occasional efforts to generalize the Harris solution to a two-dimensional situation while maintaining the exact mathematical rigor which the simple one-dimensional Harris model enjoys. The generalization includes the model by *Fadeev et al.* [1965], which depicts a series of magnetic islands, or equivalently, the filamented current layer (*Kan* [1979] also derived a similar solution but through a digressive means); the current sheet model by *Kan* [1973], which includes normal magnetic field component at the center of the current sheet and which mimics the near-Earth magnetotail current sheet; the solution by Manankova and her colleagues [*Manankova and Pudovkin*, 1996, 1999; *Manankova et al.*, 2000], which combines distinctive features from Fadeev and Kan models to depict magnetotail geometry with magnetic island structure; and the recent solution by *Brittnacher and Whipple* [2002], who adopted an earlier mathematical solution of Grad-Shrafranov-type equation by *Walker* [1915] in the context of the study of galactic structure to obtain an isolated two-dimensional X-line model.

[4] The purpose of this paper is to briefly overview the foregoing efforts and to discuss some new developments along this line. The present discussion will be focused entirely on the mathematically exact closed-form solutions constructed from the canonical momentum and total Hamiltonian of the equilibrium Vlasov equation. Specifically, the present discussion pertains to a gaussian particle distribution function with isotropic temperature. Therefore the class of solutions of the present concern can be categorized as gaussian isotropic current sheets.

[5] There are other models of one-dimensional (1-D) or two-dimensional current sheets in the context of space physical applications. For instance, *Schindler* [1972] introduced a generalized scheme to construct 1-D or 2-D isotropic current sheets with particle distribution functions that are not necessarily in the gaussian form. The resulting (generalized Grad-Shafranov) equation does not possess exact analytical solutions, however, and must be solved by numerical means or by imposing analytical approximations [*Toichi*, 1972; *Bird and Beard*, 1972; *Birn et al.*, 1975; *Zwingmann and Schindler*, 1980; *Lembege and Pellat*, 1982; *Zwingmann*, 1983; *Voigt and Moore*, 1994; *Birn and Schindler*, 2002; *Schindler and Birn*, 2002]. The advantage of this method is that by relaxing the form of distribution function from strict gaussian type, one can model various features of the current sheet equilibrium in a flexible manner. For instance, *Schindler and Birn* [2002] modeled embedded current sheet structure on the basis of such a scheme.

0148-0227/05/2003JA010308$09.00

[6] Still other alternative current sheet models are also available. For instance, *Cowley* [1978] considered anisotropic current sheet model, for which the particle distribution is the bi-Maxwellian with different perpendicular and parallel (with respect to the field) temperatures. *Cowley*'s model is built upon the notion of anisotropic 2-D current sheet discussed earlier by *Rich et al.* [1972], *Hill* [1975], and *Francfort and Pellat* [1976]. Others have also extended and commented on various aspects of anisotropic current sheet problems [*Cowley and Pellat*, 1979; *Nötzel et al.*, 1985; *Lyons and Speiser*, 1985; *Pritchett and Coroniti*, 1992a]. We note, however, that there are no known exact analytical solutions for kinetic anisotropic current sheet problem, although it is rather straightforward to discuss such a structure in terms of fluid theory [*Lui et al.*, 1995; *Yoon and Lui*, 2001].

[7] Another approach to constructing the current sheet solutions is to solve the self-consistent structure by entirely numerical means. In this regard, *Eastwood* [1972, 1974, 1975] first initiated the effort to construct the self-consistent numerical current sheet by tabulating the Speiser-type particle orbits [*Speiser*, 1965, 1967, 1968] in a model geomagnetic tail and computing the self-consistent correction to the equilibrium magnetic field from the current generated by the particles. One of the key features which distinguishes Eastwood's approach from isotropic Harris-type models or anisotropic current sheet models of Cowley type is the presence of finite dawn-to-dusk electric field, which forces the particles to drift toward the neutral sheet. Consequently, *Burkhart et al.* [1992] coined the term "forced current sheet" to designate such a class of current sheets.

[8] Beginning with the works by *Eastwood* [1972, 1974, 1975], the forced current sheets were discussed largely by means of numerical methods [*Burkhart et al.*, 1992; *Pritchett and Coroniti*, 1992b, 1993, 1994, 1995; *Holland and Chen*, 1993; *Burkhart et al.*, 1993; *Cargill et al.*, 1994; *Harold and Chen*, 1996; *Hesse et al.*, 1996; *Becker et al.*, 2001]. However, recently, semianalytical construction of the forced current sheet solutions have become available [*Kropotkin and Domrin*, 1996; *Kropotkin et al.*, 1997; *Sitnov et al.*, 2000, 2003]. In these semianalytical works, particle distribution function is constructed with not only the total Hamiltonian and canonical momentum as in Harris-type models but also with the so-called quasi-adiabatic sheet invariant. Conceptually, the model is somewhat similar to the anisotropic models of Cowley type in that the pressure anisotropy is inherent to both models, but the key difference is that the forced current sheet solution imposes a boundary condition at the outer edge of the current sheet. Specifically, it is assumed that the particle distribution in the asymptotic region features field-aligned drifts (in the deHoffmann-Teller frame), in order to represent the $\mathbf{E} \times \mathbf{B}$ motion of the particles by finite dawn-dusk electric field. The final set of equations, however, must be solved by numerical means.

[9] The class of current sheet models to be discussed in the present paper is distinct from other models briefly overviewed thus far in that we are interested in exact closed-form analytical solutions. In the subsequent discussion, we will review some of the known solutions, discuss their limitations, and also introduce some new twists on these models. The known solutions to date with geophysical application include those by *Harris* [1962], *Fadeev et al.* [1965], *Kan* [1973], *Manankova et al.* [2000], and *Brittnacher and Whipple* [2002]. Of these solutions, the models according to Harris, Fadeev, Kan, and Manankova fall into a single category which are all built upon the original solution by Harris. They represent variations on the field-reversed stretched magnetic field configuration and all reduce to Harris model in an appropriate limit. Brittnacher-Whipple model, on the other, is entirely different from the previous solutions in that their model represent an isolated X-line structure which does not reduce to Harris model in any limit. In this paper, these solutions are reviewed comprehensively, and several new solutions are proposed. The new solutions include a generalization of the Harris-Fadeev-Kan-Manankova line of model, a model for an isolated X-line alternative to that proposed by Brittnacher-Whipple, and finally a model which represents an isolated magnetic island.

2. Formal Solution to Equilibrium Vlasov Equation

[10] We are interested in a current sheet where there is no equilibrium electric potential. The class of kinetic current sheet equilibria to be discussed in the present paper is a solution of the equilibrium Vlasov kinetic equation:

$$\left[\mathbf{v}\cdot\nabla + \left(e_j/m_j c\right)(\mathbf{v}\times\mathbf{B})\cdot(\partial/\partial\mathbf{v})\right] F_j = 0,$$

$$\nabla\times\mathbf{B} = 4\pi\,\mathbf{J}/c, \quad \mathbf{J} = \sum_j e_j \int d\mathbf{v}\,\mathbf{v}\,F_j. \tag{1}$$

In what follows, let us conceive of the situation where the magnetic field vector is specified by $\mathbf{B} = \hat{\mathbf{x}}B_x(x, z) + \hat{\mathbf{z}}B_z(x, z)$, and particle distributions which depend on two spatial coordinates, $F_j = F_j(x, z, \mathbf{v})$. We are further interested in a class of distributions which satisfy the current neutrality condition along x and z axes and are charge neutral, $\Sigma_j e_j \int d\mathbf{v} v_x F_j = 0 = \Sigma_j e_j \int d\mathbf{v} v_z F_j$ and $\Sigma_j e_j \int d\mathbf{v} F_j = 0$. If we introduce the vector potential, then one can see that only the y component remains nonzero, $\mathbf{B} = \nabla \times \mathbf{A}$, where $\mathbf{A} = \hat{\mathbf{y}}A(x, z)$. Then the solution to equilibrium Vlasov equation is any function of the characteristics. Specifically, (at least) two exact characteristics,

$$P_j = m_j v_y + e_j A/c = \text{const},$$

$$H_j = m_j v^2/2 = \text{const}, \tag{2}$$

are available. These are, of course, the canonical momentum and the total Hamiltonian. From this, we may construct the solution F_j as any arbitrary function of P_j and H_j. Of infinitely many possible choices, we select the gaussian functional form, after *Harris* [1962],

$$F_j(P_j, H_j) = N_j \exp\left[-\left(H_j - V_j P_j + m_j V_j^2/2\right)/T_j\right], \tag{3}$$

where N_j, V_j, and T_j are multiplicative constants, which are related to the number density n_j, and isotropic kinetic temperature T_j, for species labeled j ($j = i$ for the ions

and e for the electrons), through the definitions, $n_j = n_{0j}\exp(e_jV_jA/cT_j)$, $v_{Tj}^2 = 2T_j/m_j$, and $n_{0j} = \pi^{3/2}v_{Tj}^3N_j$. Physically, v_{Tj} is the thermal speed, m_j and e_j are the mass and charge, respectively, and V_j corresponds to the cross-field (diamagnetic) drift speed. Note that *Schindler* [1972] proposed a scheme which does not necessarily assume the gaussian form (3). Note that the solution (3) will satisfy the (x and z component) current and charge neutrality only if $n_{0e} = n_{0i} = n_0$ and $V_i/T_i = -V_e/T_e$. We thus assume such a condition henceforth.

[11] Inserting the distribution function F_j to the field equation in (1), we obtain

$$c\nabla^2 A = -4\pi\sum_j e_j n_{0j} V_j \exp\left(e_jV_jA/cT_j\right), \tag{4}$$

where $\nabla^2 = \partial^2/\partial x^2 + \partial^2/\partial z^2$. Let us introduce two constants, $B_0^2 = 8\pi n_0(T_e + T_i)$ and $L = 2cT_i/(eB_0V_i)$, where B_0 will turn out to be the asymptotic ($z^2 \to \infty$) magnetic field strength and L is the characteristic scale length associated with the current sheet. We further introduce dimensionless quantities,

$$X = x/L, \quad Z = z/L, \quad \Psi = -A/(LB_0). \tag{5}$$

Then the equilibrium Ampere's law (Grad-Shafranov equation) becomes

$$\partial^2\Psi/\partial X^2 + \partial^2\Psi/\partial Z^2 = e^{-2\Psi}. \tag{6}$$

Note that the density is given in terms of Ψ by $n = n_i = n_e = n_0e^{-2\Psi}$. Thus the problem of obtaining exact two-dimensional current sheet equilibrium solutions boils down to solving the above Grad-Shafranov equation for $\Psi(X, Z)$.

[12] The general solution in terms of complex variable, $\zeta = X + iZ$, was obtained by *Walker* [1915]. He first notes that any complex function of the form $f(\zeta) = g(\zeta) + h(\zeta^*)$, where the asterisk denotes the complex conjugate, satisfies the homogeneous equation, $\partial^2 f/\partial X^2 + \partial^2 f/\partial Z^2 = 0$. He then proceeds to write down an inhomogeneous solution, $\Psi = (1/2)\ln\{-f^2/[(\partial f/\partial X)^2 + (\partial f/\partial Z)^2]\}$, the validity of which can easily be checked by simply inserting the above solution to (6). For a specific choice of $h(\zeta^*)$, Walker selects $h(\zeta^*) = 1/g^*(\zeta)$. Then by writing $g(\zeta) = u(X, Z) + iv(X, Z)$, where u and v are real functions, one can show that $f^2 = (1 + u^2 + v^2)/(u - iv)^2$, $(\partial f/\partial X)^2 = (\partial f/\partial Z)^2 = -4(u_X^2 + v_Z^2)/(u - iv)^2$. Here, $u_X = \partial u/\partial X$ and $v_X = \partial v/\partial X$. Since $\partial v/\partial X = -\partial u/\partial Z$ and $\partial u/\partial X = \partial v/\partial Z$, Walker thus obtains the formal solution to (6) as follows:

$$e^{-2\Psi} = 4|g'|^2/\left(1 + |g|^2\right)^2, \tag{7}$$

where $g' = dg(\zeta)/d\zeta$. This result, which forms the basis for the construction of specific current sheet models discussed next, is also widely used in the theory of relativistic beam equilibria [*Benford and Book*, 1971]. All that remains is the choice of specific functional form for the generating function $g(\zeta)$. Of course there are infinite varieties of $g(\zeta)$ in a purely mathematical sense, but not all choices will turn out to be useful from a physical perspective. In the next section, we review the known solutions to date with geophysical applications and suggest alternative solutions.

3. Specific Examples of Exact Current Sheet Equilibria

3.1. Harris Solution

[13] Harris model [*Harris*, 1962] can be obtained if we choose the generating function as

$$g(\zeta) = \exp(i\zeta). \tag{8}$$

Then, the specific solution becomes

$$n/n_0 = e^{-2\Psi} = \mathrm{sech}^2 Z, \quad \Psi = -A/LB_0 = \ln(\cosh Z). \tag{9}$$

This is a one-dimensional model, since $B_z = 0$ and $B_x = B_0\tanh Z$. The profile of the cross-field current across Z is dictated by the density profile, $J_y/[en_0V_i(1 + T_e/T_i)] = \mathrm{sech}^2 Z$, but the current density is uniform across X.

3.2. Fadeev Solution

[14] Fadeev model [*Fadeev et al.*, 1965] represents a filamented current sheet, or equivalently, an infinite chain of magnetic X-lines. The generating function which results in the Fadeev solution is

$$g(\zeta) = f + \sqrt{1+f^2}\,\exp(i\zeta). \tag{10}$$

When $f = 0$, of course, one recovers the Harris model. With (10), the solutions are

$$e^{-2\Psi} = \frac{n}{n_0} = \frac{J_y}{en_0V_i(1 + T_e/T_i)} = \frac{1}{\left(f\cos X + \sqrt{1+f^2}\,\cosh Z\right)^2},$$

$$\Psi = -\frac{A}{LB_0} = \ln\left(f\cos X + \sqrt{1+f^2}\,\cosh Z\right). \tag{11}$$

Figure 1 shows the plot of normalized vector potential, $\Psi = -A/B_0L$, for Fadeev model. Two values of f are used, namely, $f = 0.5$ and 5. Note the filamented current density structure along X axis, and the nested closed magnetic field lines (O lines or magnetic islands). Between every pair of magnetic islands is the magnetic null, or X point.

3.3. Kan Solution

[15] In the original Kan's model [*Kan*, 1973], the author employed two adjustable parameters, but it is essentially a one-parameter model. The generating function for Kan solution is

$$g(\zeta) = \exp\left(i\zeta - \frac{ib}{\zeta}\right). \tag{12}$$

In the original Kan's paper the denominator within the argument of the exponential function on the right-hand side is replaced by $\zeta - a$. However, the parameter a simply shifts the entire solution along X axis and since Kan applied his solution over a restricted 2-D domain only, we could simply put $a = 0$, and instead limit the applicability of the

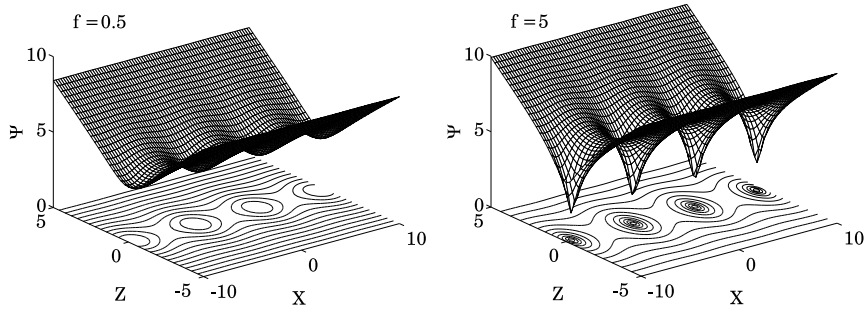

Figure 1. Normalized vector potential, $\Psi = -A/B_0L$ in Fadeev model.

solutions in accordance with Kan's original intention. With (12), the desired solution is

$$\Psi = \ln \frac{\cosh[Z(1 + b/R^2)]}{\sqrt{(1 + b/R^2)^2 - 4bZ^2/R^4}}, \quad R^2 = X^2 + Z^2. \tag{13}$$

In Figure 2 the normalized vector potential Ψ in Kan model, computed for $b = 0.5$ is shown. Here, we have intentionally plotted the model over an entire XZ-plane in order to emphasize the mathematical structure of Ψ near the origin. The right-hand panel shows the details of the behavior of the model near the origin, which is peculiar owing to the mathematical structure of the argument of the logarithmic function in (13). Kan model has three singular points near the origin, $(X, Z) = (0, 0)$ and $(X, Z) = (0, \pm\sqrt{b})$. For this reason, the model should be applied to only a portion of the (X, Z) space which excludes the origin or its immediate vicinity. How close one wishes to get to the origin is an entirely arbitrary choice, and in the original Kan model this choice is controlled by the parameter a. In the present discussion, however, we simply avoid the origin by choosing to apply the solution to a partial domain where X is greater (or less) than a certain prescribed value.

[16] In Figure 3, we therefore applied Kan model to positive X space corresponding to $X > 0.5$. Two choices of the parameter b are used, namely, $b = 0.5$ and 2. Kan model is characterized by flaring magnetic field for high values of Z regardless of X. The flaring behavior becomes more emphasized near the origin and for increasing b value. Because of the high flaring angle near the origin, Kan model has a limitation in representing the near-Earth dipole-like magnetic field behavior. Later, however, we will suggest a possible remedy to this problem.

3.4. Manakova Solution

[17] Manankova and her colleagues [*Manankova and Pudovkin*, 1996, 1999; *Manankova et al.*, 2000] combined the aspects of both the Fadeev and Kan models and came up with the generating function of the form

$$g(\zeta) = f + \sqrt{1 + f^2}\, \exp\left(i\zeta - \frac{ib}{\zeta - a}\right). \tag{14}$$

In the above expression the shifted denominator $\zeta - a$ now makes a difference, since the parameter a can be adjusted to place the magnetic islands relative to the divergence points. The result is

$$\Psi = \ln \frac{f \cos X_* + \sqrt{1 + f^2}\, \cosh Z_*}{\sqrt{W}},$$

$$X_* = X - \frac{b\,(X - a)}{R^2}, \quad Z_* = Z\left(1 + \frac{b}{R^2}\right),$$

$$W = \left(1 + \frac{b}{R^2}\right)^2 - \frac{4bZ^2}{R^4}, \quad R^2 = (X - a)^2 + Z^2. \tag{15}$$

[18] As with Kan model, the above solution possesses various singularities near the origin. Specifically, the singularities occur for $(X, Z) = (a, 0)$ and $(X, Z) = (a, \pm\sqrt{b})$. The

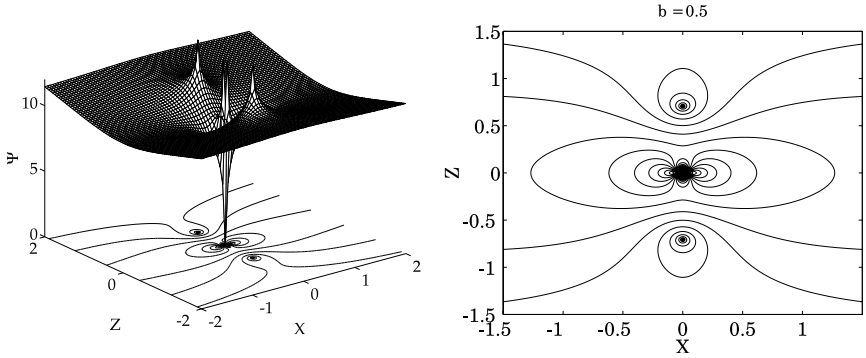

Figure 2. Normalized vector potential, Ψ, in Kan model, computed for $b = 0.5$. The right-hand panel shows the details of the model near the origin.

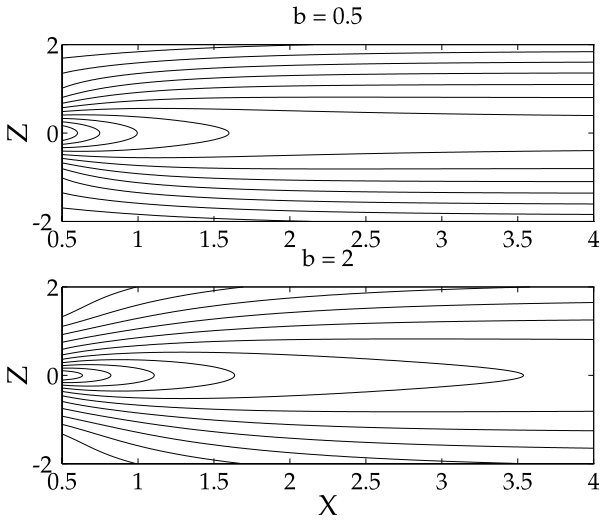

Figure 3. Application of Kan model to positive X space corresponding to $X > 0.5$. Four values of the b parameter are used, namely, $b = 0.5$, 2, 5, and 10.

plot of Ψ in the region which encompasses these singularities reveals that it is very similar to that of Kan model (not shown). In Figure 4, we plot the above solution for $a = 0$, $b = 2$, and for two values of f corresponding to $f = 0.1$ and $f = 0.5$. Note that the case for $f = 0.1$ describes a stretched current sheet in the near-Earth region, while the choice of $f = 0.5$ yields stationary magnetic island structure down the tail.

[19] In Kan's model the choice of a simply meant the translation of the whole structure along X axis. In Manankova's model, the island structure is fixed along X axis, and thus the different choice of a implies that the relative distance between the island structure and the singular points changes. Therefore the parameter a can be adjusted to place the location of the magnetic islands in relation to the origin.

3.5. Generalization of Harris-Fadeev-Kan-Manankova Solution

[20] In the model by Kan and Manankova, the divergence at the point $(X, Z) = (a, 0)$ is controlled by the factor $ib/(\zeta - a)$ in the generating function. As such, the singularity scale as $\mathcal{O}(R^{-1})$ near the point $(X, Z) = (a, 0)$. Here $R = \sqrt{(X-a)^2+Z^2}$. In the following model, we seek to modify the $\mathcal{O}(R^{-1})$ divergence behavior by allowing an arbitrary power. Thus we suggest a new generating function which has the form

$$g(\zeta) = f + \sqrt{1+f^2}\,\exp\left(i\zeta - \frac{ib}{(\zeta-a)^k}\right). \tag{16}$$

If we take $k = 1$, then we recover Manankova's model. Taking the derivative with respect to the argument, we obtain

$$g'(\zeta) = i\sqrt{1+f^2}\left(1+\frac{kb}{(\zeta-a)^{k+1}}\right)\exp\left(i\zeta - \frac{ib}{(\zeta-a)^k}\right). \tag{17}$$

If we define

$$R = \sqrt{(X-a)^2+Z^2}, \quad \theta = \tan^{-1}\frac{Z}{X-a}, \tag{18}$$

then we arrive at the desired solution,

$$\Psi = \ln\frac{f\cos X_* + \sqrt{1+f^2}\,\cosh Z_*}{\sqrt{W}}$$

$$X_* = a + R\cos\theta - \frac{b\cos k\theta}{R^k}, \quad Z_* = R\sin\theta + \frac{b\sin k\theta}{R^k},$$

$$W = \left(1+\frac{kb}{R^{k+1}}\right)^2 - \frac{4kb}{R^{k+1}}\sin^2\frac{(k+1)\theta}{2}. \tag{19}$$

This is a direct generalization of Manankova's model which is built upon the earlier solutions by Harris, Fadeev, and Kan.

[21] To see the difference between the present new model (19) and the earlier Kan or Manakova models, let us consider the case of $f = 0$ (that is, Kan model). For the sake of simplicity, let us place the singular point at the origin, $a = 0$, and restrict ourselves to $b = 2$. With these choices of parameters, we are ready to compare the early model with the present generalized model. As we noted already, the case of $k = 1$ corresponds to the model considered by Kan. This case is shown on the top panel of Figure 5. In contrast, the bottom panel shows the case of $k = 0.1$. As one can see, the divergent behavior near the singular point and the flaring angle associated with the magnetic field lines are drastically different in the two cases. The choice of $k = 0.1$ renders the model magnetic field lines which bear more realistic resemblance to the actual magnetotail geometry.

3.6. Brittnacher-Whipple Solution

[22] The solution by *Brittnacher and Whipple* [2002] is an entirely different model when compared with the Harris

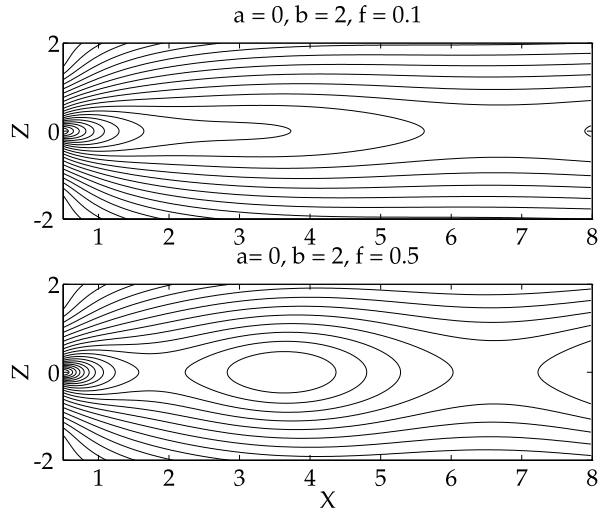

Figure 4. Contour plot of normalized vector potential Ψ in Manankova model, computed for $a = 0$, $b = 2$, and for $f = 0.1$ (left) and $f = 0.5$ (right).

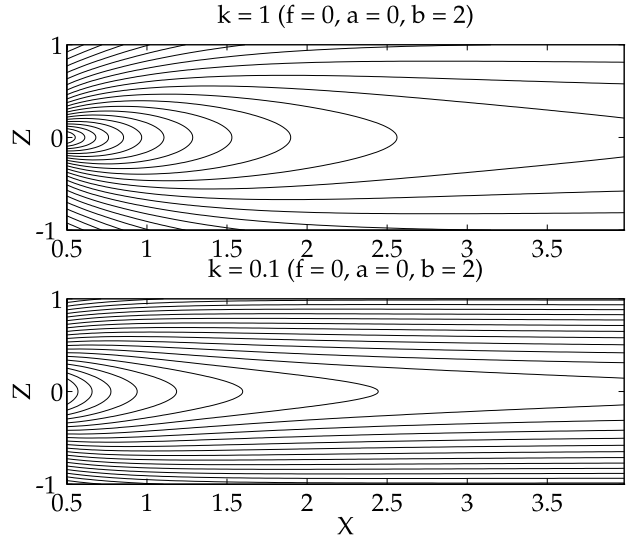

Figure 5. Comparison of the Kan model (13) and the present generalized model (19). For both cases, we choose $f = 0$ (no magnetic island structure), $a = 0$ (singularity at the origin), $b = 2$. The left-hand panel ($k = 1$) corresponds to Kan model, while the right-hand panel ($k = 0.1$) represents the present generalized model.

model. It does not reduce to the Harris solution in any limiting situation, and the model depicts an isolated pair of currents parallel to each other containing magnetic X point encompassed by a pair of magnetic islands. In a mathematical sense, their solution is identical to one of Walker's several solutions [*Walker*, 1915]. The choice of generating function $g(\zeta)$ in Walker-Brittnacher-Whipple (WBW) model is an exponential function of not $\zeta = X + iZ$ itself but is an exponential functional of a function of ζ, namely,

$$g(\zeta) = \exp[-\beta\rho(\zeta)]. \tag{20}$$

The choice $\rho(\zeta)$ is made in accordance with the definition of elliptic coordinate transformation,

$$\zeta = \alpha\cosh\rho, \tag{21}$$

or, equivalently,

$$\rho(\zeta) = \cosh^{-1}(\zeta/\alpha) = \ln\frac{\zeta \pm \sqrt{\zeta^2 - \alpha^2}}{\alpha}. \tag{22}$$

The detailed derivation of the solution is given in the paper by *Brittnacher and Whipple* [2002]. The result can be summarized as follows:

$$\Psi = \ln\frac{\sqrt{r_+ r_-}\,\cosh(\beta\xi)}{\beta},$$

$$r_\pm = \sqrt{(X \pm \alpha)^2 + Z^2},$$

$$\xi = \ln\left(\tau + \sqrt{\tau^2 - 1}\right), \quad \tau = \frac{r_+ + r_-}{2\alpha}. \tag{23}$$

The parameter α determines the relative location of the pair of parallel currents, while the parameter β determines the shape (the ellipticity) of the magnetic islands. In WBW model, the current density at loci $(X, Z) = (\pm\alpha, 0)$ becomes infinite. Thus in applying this solution it is prudent to exclude these points.

[23] In Figure 6 we show the contour plot of Ψ as given by (23). Since the parameter α simply determines the relative distance between the two centers of the parallel currents, we do not vary this parameter but choose a fixed value $\alpha = 2$. Thus the current density maximizes at $X = \pm 2$. The parameter β determines the ellipticity of the magnetic islands. For low values, the island structure becomes O-shaped, while for high values of β the islands becomes elongated. In Figure 6 we show two values, $\beta = 0.5$ and $\beta = 5$. Note that Brittnacher and Whipple restricted their model to the vicinity of X point between the two magnetic islands which excludes the pair of singular currents, but the present plot intentionally shows the entire structure.

3.7. Walker's Current Rod Solution

[24] In the paper by *Walker* [1915], whose original intended application is in galactic structure not plasma physics, the author discusses a number of possible generating functions. One of them can be translated, in the plasma physical context, as a current rod solution (i.e., cylindrical current distribution of infinite length). The generating function for such equilibria is

$$g(\zeta) = \zeta^\nu. \tag{24}$$

The density $n/n_0 = e^{-2\Psi}$ and the vector potential $A_y/(B_0 L) = -\Psi$ are obtained from the relation

$$e^{-2\Psi} = \frac{4\nu^2}{R^2\left(R^\nu + R^{-\nu}\right)^2}, \qquad R = \sqrt{X^2 + Z^2}. \tag{25}$$

If $\nu > 1$, then the density $n/n_0 = e^{-2\Psi}$ at the core $R = 0$ drops down to zero. On the other hand, for $\nu < 1$, the density

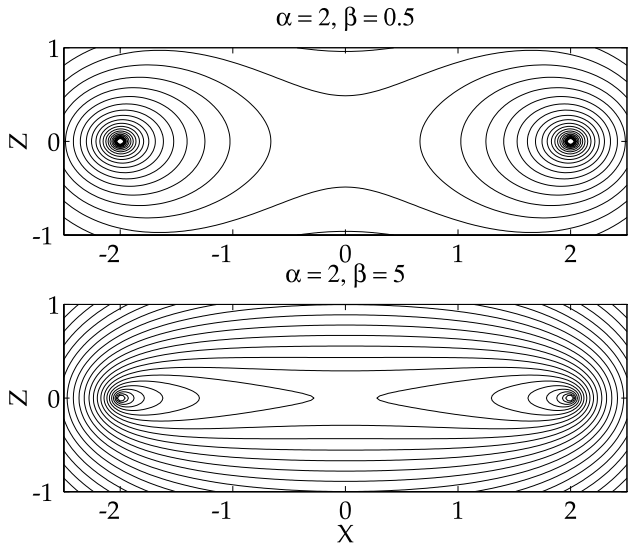

Figure 6. Mesh and contour plots of Ψ in Walker-Brittnacher-Whipple (WBW) model. The parameter α determines the location of the parallel currents. We chose $\alpha = 2$ and thus the current density maximizes at $X = \pm 2$. The parameter β determines the shape of the magnetic islands. We chose two values, $\beta = 0.5$ and $\beta = 5$.

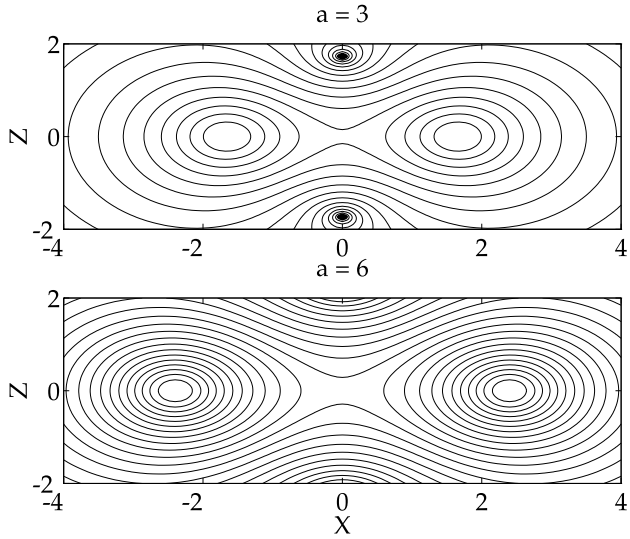

Figure 7. Normalized vector potential Ψ in alternative X-line model. The case of $a = 3$ shows the presence of singular antiparallel currents just outside the X-line. The choice of $a = 6$ pushes the singular currents to outside of the plotting range. The distinguishing feature of the present model is that the cross-field currents at the O-points are finite.

diverges at $R = 0$. Thus the case of $\nu = 1$ is a peculiar case where the current rod has a nondivergent current density at the core. In the subsequent discussions, we will introduce a couple of new twists on this solution (i.e., variations on $\nu = 1$ case).

3.8. Equilibrium Structure Containing an Isolated X-Line

[25] In the *Brittnacher and Whipple* [2002] model the current equilibrium structure containing an X-line is characterized by a pair of parallel currents whose density diverges at the two current centers. The model to be discussed next is an alternative X-line model where the current density at the center of magnetic islands is finite. However, the drawback of the present model is that it contains a pair of singular currents flowing in the opposite direction just outside the X-line, as will be shown. The generating function for our alternative X-line model is

$$g(\zeta) = \zeta - a/\zeta. \tag{26}$$

The density $n/n_0 = e^{-2\Psi}$ and the vector potential $A_y/(B_0L) = -\Psi$ can be computed from

$$\Psi = \ln \frac{(R^2 + a)^2 + R^2 - 4aX^2}{2\left[(R^2 + a)^2 - 4aZ^2\right]^{1/2}}, \tag{27}$$

where $R^2 = X^2 + Z^2$.

[26] Figure 7 plots the normalized vector potential Ψ for the present alternative X-line model. The case of $a = 3$ clearly shows the presence of singular antiparallel currents just outside the X-line. The application of the present model therefore must exclude these singularities, just as Brittnacher and Whipple avoided the singularities in applying their model. In this regard, the choice of $a = 6$, for instance, results in the singular currents being placed outside of the plotting range. The distinguishing feature of the present model in contrast to Brittnacher-Whipple model is that as noted already, the cross-field currents at the O-lines are finite.

3.9. An Isolated Magnetic Island Equilibrium

[27] Walker's current rod equilibrium can be interpreted as a simple example of an isolated magnetic island structure whose cylindrical current density has a circular cross section. However, it can be generalized to a magnetic island structure with an elongated cross section. Such a structure can be thought of as a merged state of two magnetic O-lines. It is known that a pair of magnetic islands with an X-line between them (such as that discussed in the previous subsection) can be unstable to the coalescence instability [*Finn and Kaw*, 1977; *Pritchett and Wu*, 1979; *Bhattacharjee et al.*, 1983; *Schumacher and Kliem*, 1997]. The isolated island structure to be discussed next can be considered as an end state of such a coalescence process. We propose a new generating function for such a structure as given by

$$g(\zeta) = \zeta/\left(1 - a^2\zeta^2\right), \tag{28}$$

with the solution

$$\Psi = \frac{1}{2}\ln\frac{S\left(S + R^2\right)^2}{2T},$$

$$S = \left(1 - a^2R^2\right)^2 + (2aZ)^2, \quad T = \left(1 - a^4R^4\right)^2 + \left(4a^2XZ\right)^2, \tag{29}$$

with $R^2 = X^2 + Z^2$ as before. Figure 8 shows the plot of Ψ for two different choices of a corresponding to $a = 0.4$ and $a = 0.1$.

4. Conclusions

[28] In the present paper we have discussed a class of exact two-dimensional kinetic current sheet equilibria. The general

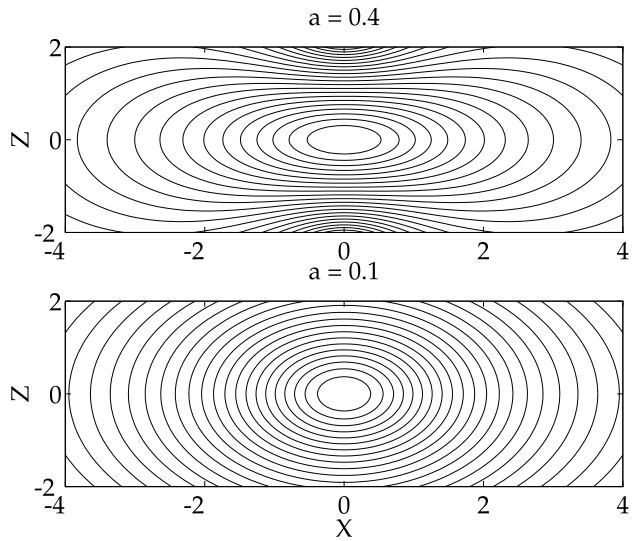

Figure 8. Plot of Ψ for two different choices of a corresponding to $a = 0.4$ and $a = 0.1$.

solution to the two-dimensional Grad-Shafranov equation (equation (6)) was first obtained by Walker [*Walker*, 1915], whose intended application was to galactic structure. However, his method can be directly translated to plasma physical application. The specific solution thus becomes a matter of the choice for the generating function $g(\zeta)$. Apparently, there are infinite choices, but not every solution yields physically meaningful or useful mathematical form. The known solutions to date with geophysical application include the Harris model [*Harris*, 1962], Fadeev model [*Fadeev et al.*, 1965; *Kan*, 1979], Kan model [*Kan*, 1973], Manankova model [*Manankova and Pudovkin*, 1996, 1999; *Manankova et al.*, 2000], and Walk-Brittnacher-Whipple model [*Walker*, 1915; *Brittnacher and Whipple*, 2002]. Of these, Fadeev, Kan, and Manankova solutions are all variations and generalization of Harris model. In contrast, the Walk-Brittnacher-Whipple model does not reduce to the Harris model.

[29] We have generalized the Harris-Fadeev-Kan-Manankova line of model by allowing the singularity associated with the argument of the exponential function in Kan and Manankova model to scale by an arbitrary power (section 3.5). We have also presented a model of a pair of magnetic islands with an X-line in between (section 3.8), and a model which represents an isolated magnetic island (section 3.9). The latter two new models are essentially variations on Walker's two-dimensional current rod solution.

[30] On the basis of specific examples examined in the present paper, we conclude that exact two-dimensional solutions of current structure can be constructed with enough flexibility to model a variety of physical features relevant to geophysical application, such as magnetic neutral lines, magnetic island structure, near-Earth magnetotail-like behavior, etc. However, we also conclude that sometimes these models possess various singularities such that the actual applications of the models must exclude these singular points. As long as one excludes singularities, the exact 2-D models are extremely useful in that they satisfy exact equilibrium force balance conditions within the restricted domain.

[31] **Acknowledgments.** This research was supported by NASA grant NAG5-10475 to Johns Hopkins University.

[32] Lou-Chuang Lee thanks Daniel Holland and the other two reviewers for their assistance in evaluating this paper.

References

Becker, U., T. Neukirch, and K. Schindler (2001), On the quasistatic development of thin current sheets in magnetotail-like magnetic fields, *J. Geophys. Res.*, *106*, 3811.

Benford, G., and D. L. Book (1971), Relativistic beam equilibria, in *Advances in Plasma Physics*, vol. 4, edited by A. Simon and W. B. Thompson, p. 125, Wiley-Interscience, New York.

Bhattacharjee, A., F. Brunel, and T. Tajima (1983), Magnetic reconnection driven by the coalescence instability, *Phys. Fluids*, *26*, 3332.

Bird, M. K., and D. B. Beard (1972), The self-consistent geomagnetic tail under static conditions, *Planet. Space Sci.*, *20*, 2057.

Birn, J., R. Sommer, and K. Schindler (1975), Open and closed magnetospheric tail configurations and their stability, *Astrophys. Space Sci.*, *35*, 389.

Birn, J., and K. Schindler (1992), Thin current sheets in the magnetotail and the loss of equilibrium, *J. Geophys. Res.*, *107*(A7), 1117, doi:10.1029/2001JA000291.

Brittnacher, M., and E. C. Whipple (2002), Extension of the Harris magnetic field model to obtain exact, two-dimensional, self-consistent X point structures, *J. Geophys. Res.*, *107*(A2), 1022, doi:10.1029/2001JA000216.

Burkhart, G. R., J. F. Drake, P. B. Dusenbery, and T. W. Speiser (1992), A particle model for magnetotail neutral sheet equilibria, *J. Geophys. Res.*, *97*, 13,799.

Burkhart, G. R., P. B. Dusenbery, T. W. Speiser, and R. E. Lopez (1993), Hybrid simulations of thin current sheets, *J. Geophys. Res.*, *98*, 21,373.

Burton, M. E., N. U. Crooker, G. L. Siscoe, and E. J. Smith (1994), A test of source-surface model predictions of heliospheric current sheet inclination, *J. Geophys. Res.*, *99*, 1.

Cargill, P. G., J. Chen, and J. B. Holland (1994), One-dimensional hybrid simulations of current sheets in the quiet magnetotail, *Geophys. Res. Lett.*, *21*, 2251.

Cowley, S. W. H. (1978), The effect of pressure anisotropy on the equilibrium structure of magnetic current sheets, *Planet. Space Sci.*, *26*, 1037.

Cowley, S. W. H., and R. Pellat (1979), A note on adiabatic solutions of the one-dimensional current sheet problem, *Planet. Space Sci.*, *27*, 265.

Eastwood, J. W. (1972), Consistency of fields and particle motion in the 'Speiser' model of the current sheet, *Planet. Space Sci.*, *20*, 1555.

Eastwood, J. W. (1974), The warm current sheet model and its implications on the temporal behavior of the geomagnetic tail, *Planet. Space Sci.*, *22*, 1641.

Eastwood, J. W. (1975), Some properties of the current sheet in the geomagnetic tail, *Planet. Space Sci.*, *23*, 1.

Fadeev, V. M., I. F. Kvartskhava, and N. N. Komarov (1965), Self-focusing of the local plasma currents (in Russian), *Nucl. Fusion*, *5*, 202.

Finn, J. M., and P. K. Kaw (1977), Coalescence instability of magnetic islands, *Phys. Fluids*, *20*, 72.

Francfort, P., and R. Pellat (1976), Magnetic merging in collisionless plasmas, *Geophys. Res. Lett.*, *3*, 433.

Harold, J. B., and J. Chen (1996), Kinetic thinning in one-dimensional self-consistent current sheets, *J. Geophys. Res.*, *101*, 24,899.

Harris, E. G. (1962), On a plasma sheath separating regions of oppositely directed magnetic field, *Nuovo Cimento*, *23*, 116.

Hesse, M., D. Winske, M. Kuznetsova, J. Birn, and K. Schindler (1996), Hybrid modeling of the formation of thin current sheets in magnetotail configurations, *J. Geomagn. Geoelectr.*, *48*, 749.

Hill, T. W. (1975), Magnetic merging in a collisionless plasma, *J. Geophys. Res.*, *80*, 4689.

Holland, D. L., and J. Chen (1993), Self-consistent current sheet structures in the quiet-time magnetotail, *Geophys. Res. Lett.*, *20*, 1775.

Kan, J. R. (1973), On the structure of the magnetotail current sheet, *J. Geophys. Res.*, *78*, 3773.

Kan, J. R. (1979), Nonlinear tearing structures in equilibrium current sheet, *Planet. Space Sci.*, *27*, 351.

Kropotkin, A. P., and V. I. Domrin (1996), Theory of a thin one-dimensional current sheet in collisionless space plasma, *J. Geophys. Res.*, *101*, 19,893.

Kropotkin, A. P., H. V. Malova, and M. I. Sitnov (1997), Self-consistent structure of a thin anisotropic current sheet, *J. Geophys. Res.*, *102*, 22,099.

Lembege, B., and R. Pellat (1982), Stability of a thick two-dimensional quasi-neutral sheet, *Phys. Fluids*, *25*, 1995.

Lui, A. T. Y., C.-L. Chang, and P. H. Yoon (1995), Preliminary nonlocal analysis of cross-field current instability for substorm expansion onset, *J. Geophys. Res.*, *100*, 19,147.

Lyons, L. R., and T. W. Speiser (1985), Ohm's law for a current sheet, *J. Geophys. Res.*, *90*, 8543.

Manankova, A. V., and M. I. Pudovkin (1996), Energy characteristics of a two-dimensional current-carrying plasma, *Geomagn. Aeron.*, *36*, 8.

Manankova, A. V., and M. I. Pudovkin (1999), The description of a two-dimensional current-carrying plasma sheet in the hydrodynamic approximation of a single-component plasma model, *Geomagn. Aeron.*, *39*, 42.

Manankova, A. V., M. I. Pudovkin, and A. V. Runov (2000), Stationary configurations of the two-dimensional current-carrying plasma sheet: Exact solutions, *Geomagn. Aeron.*, *40*, 430.

Ness, N. F. (1965), The Earth's magnetic tail, *J. Geophys. Res.*, *70*, 2989.

Ness, N. F. (1987), Magnetotail research: The early years, in *Magnetotail Physics*, edited by A. T. Y. Lui, p. 11–20, Johns Hopkins Univ. Press, Baltimore, Md.

Nötzel, A., K. Schindler, and J. Birn (1985), On the cause of approximate pressure isotropy in the quiet near-Earth plasma sheet, *J. Geophys. Res.*, *90*, 8293.

Pritchett, P. L., and F. V. Coroniti (1992a), Interaction of reflected ions with the firehose marginally stable current sheet: Implications for plasma sheet convection, *Geophys. Res. Lett.*, *19*, 1631.

Pritchett, P. L., and F. V. Coroniti (1992b), Formation and stability of the self-consistent one-dimensional current sheet, *J. Geophys. Res.*, *97*, 16,773.

Pritchett, P. L., and F. V. Coroniti (1993), A radiating one-dimensional current sheet configuration, *J. Geophys. Res.*, *98*, 15,355.
Pritchett, P. L., and F. V. Coroniti (1994), Convection and the formation of thin current sheets in the near-Earth plasma sheet, *Geophys. Res. Lett.*, *21*, 1587.
Pritchett, P. L., and F. V. Coroniti (1995), Formation of thin current sheets during plasma sheet convection, *J. Geophys. Res.*, *21*, 23,551.
Pritchett, P. L., and C. C. Wu (1979), Coalescence of magnetic islands, *Phys. Fluids*, *22*, 2140.
Rich, F. J., V. M. Vasyliunas, and R. A. Wolf (1972), On the balance of stresses in the plasma sheet, *J. Geophys. Res.*, *77*, 4670.
Schindler, K. (1972), A self-consistent theory of the tail of the magnetosphere, in *Earth's Magnetospheric Processes*, edited by B. M. McComas, p. 200, D. Reidel, Norwell, Mass.
Schindler, K., and J. Birn (2002), Models of two-dimensional embedded thin current sheets from Vlasov theory, *J. Geophys. Res.*, *107*(A8), 1193, doi:10.1029/2001JA000304.
Schumacher, J., and B. Kliem (1997), Coalescence of magnetic islands including anomalous resistivity, *Phys. Plasmas*, *4*, 3533.
Siscoe, G. L., J. A. Slavin, E. J. Smith, B. T. Tsurutani, D. E. Jones, and D. A. Mendis (1986), Statics and dynamics of Giacobini-Zinner magnetic tail, *Geophys. Res. Lett.*, *13*, 287.
Sitnov, M. I., L. M. Zelenyi, H. V. Malova, and A. S. Sharma (2000), Thin current sheet embedded within a thicker plasma sheet: Self-consistent kinetic theory, *J. Geophys. Res.*, *105*, 13,029.
Sitnov, M. I., P. N. Guzdar, and M. Swizdak (2003), A model of the bifurcated current sheet, *Geophys. Res. Lett.*, *30*(13), 1712, doi:10.1029/2003GL017218.
Solanki, S. K., A. Lagg, J. Woch, N. Krupp, and M. Collados (2003), Three-dimensional magnetic field topology in a region of solar coronal heating, *Nature*, *425*, 692.
Speiser, T. W. (1965), Particle trajectories in model current sheets, *J. Geophys. Res.*, *70*, 4219.
Speiser, T. W. (1967), Particle trajectories in model current sheets: 2. Applications to auroras using a geomagnetic tail model, *J. Geophys. Res.*, *72*, 3919.
Speiser, T. W. (1968), On the uncoupling of parallel and perpendicular particle motion in a neutral sheet, *J. Geophys. Res.*, *73*, 1112.
Toichi, T. (1972), Two-dimensional equilibrium solution of the plasma sheet and its application to the problem of the tail magnetosphere, *Cosmic Electrodyn.*, *3*, 81.
Voigt, G.-H., and B. D. Moore (1994), A note on two-dimensional asymptotic magnetotail equilibria, *J. Geophys. Res.*, *99*, 5943.
Walker, G. W. (1915), Some problems illustrating the forms of nebulae, *Proc. R. Soc. London, Ser. A*, *91*, 410.
Yoon, P. H., and A. T. Y. Lui (2001), Stabilization of lower-hybrid drift instability in the magnetotail by finite north-south magnetic field component and destabilization by sheared cross-field flow, *J. Geophys. Res.*, *106*, 13,203.
Zwingmann, W. (1983), Self-consistent magnetotail theory: Equilibrium structures including arbitrary variation along the tail axis, *J. Geophys. Res.*, *88*, 9101.
Zwingmann, W., and K. Schindler (1980), Magnetic islands in the quiet magnetotail, *Geophys. Res. Lett.*, *7*, 909.

A. T. Y. Lui, Johns Hopkins University Applied Physics Laboratory, Laurel, MD 20723, USA. (tony.lui@jhuapl.edu)
P. H. Yoon, Institute for Physical Science and Technology, University of Maryland, College Park, MD 20742, USA. (yoonp@ipst.umd.edu)